A&A 442, 323–329 (2005)
DOI: 10.1051/0004-6361:20053299

Astronomy & Astrophysics

Photometry of umbral dots

M. Sobotka[1] and A. Hanslmeier[2]

[1] Astronomical Institute, Academy of Sciences of the Czech Republic, 25165 Ondřejov, Czech Republic
e-mail: msobotka@asu.cas.cz
[2] Institut für Physik, IGAM, Karl-Franzens University, Universitätsplatz 5, 8010 Graz, Austria
e-mail: arnold.hanslmeier@uni-graz.at

Received 25 April 2005 / Accepted 17 June 2005

ABSTRACT

Until now, the size of umbral dots has been considered to be below the resolution limit of large solar telescopes. We analyze observations of two sunspots and two pores, acquired in September 2003 with the new 1-m Swedish Solar Telescope, La Palma. White-light images with a resolution better than 0.″15 were taken simultaneously in blue (451 nm) and red (602 nm) wavelength bands. They were corrected for scattered light and restored for the instrumental profile of the telescope. Intensities, diameters and positions of umbral dots were measured in aligned pairs of images in the blue and red wavelength band. We find that observed intensities of umbral dots are correlated with local intensities of umbral background. On average, UDs are by about 1000 K hotter than the coolest area in the umbra and by 500–1000 K cooler than the undisturbed photosphere. Individual UDs may reach or exceed the average photospheric brightness and temperature. Histograms of observed diameters peak at 0.″23 (170 km). This indicates that the majority of umbral dots are spatially resolved with the 1-m telescope. The mean nearest-neighbour distance between umbral dots is 0.″4 and their average observed filling factor is 9%. The method of two-colour photometry is discussed and applied to obtain average "true" intensities and diameters. About 50% of umbral dots are brighter than the quiet photosphere and the average "true" diameter of umbral dots is 100 km. However, the latter results might be influenced by systematic errors of the method.

Key words. Sun: sunspots – instrumentation: high angular resolution

1. Introduction

Sunspots and pores are formed by magnetic flux tubes emerging from the convection zone to the solar atmosphere. The suppresion of convective motion perpendicular to the magnetic field causes these structures to be cooler than the undisturbed regions of the Sun (Biermann 1941). However, the complete suppression of convection cannot explain the observed brightness of umbrae. They are heated from the underlying convective zone by magnetoconvection (e.g. Hurlburt et al. 2000; Thomas & Weiss 2004, and references therein) or by intrusion of thin columns of hot field-free plasma (Parker 1979; Choudhuri 1992). This heat input manifests in the form of light bridges and of umbral dots (UDs), tiny bright features observed and named by Danielson (1964). Light bridges and UDs are also observed in pores. Their characteristics are similar to those in sunspot umbrae (Sobotka et al. 1999).

Only the largest solar telescopes located at the best sites can be used to observe UDs, often at the resolution limit. Since UDs are very small and both the instrument and the turbulent terrestrial atmosphere degrade the image, it can be expected that "true" intensities of UDs are larger and "true" diameters smaller than the observed ones. Observations with the old 0.5-m Swedish Vacuum Solar Telescope, La Palma, have shown a strong increase of the number of UDs with decreasing diameter down to the resolution limit of 0.″25 (Sobotka et al. 1997). A similar result was obtained by Tritschler & Schmidt (2002b) who, using the phase-diversity technique, corrected their observations for instrumental and atmospheric point spread functions thus achieving the cut-off limit of the 0.7-m Vacuum Tower Telescope at Tenerife. No typical observed diameter of UDs was found and thus most UDs remained unresolved. The observed intensity of UDs seems to be related to the intensity of the local umbral background (Sobotka et al. 1993; Denker 1998; Tritschler & Schmidt 2002b). On average, UDs are 1.3–1.5 times brighter than the background.

The "true" intensities and diameters of UDs are needed for physical modelling of plasma processes in the umbra to explain the umbral heating and the complex observed structure, and also for restrictions used in inversion problems when deriving the magnetic field and line-of-sight velocity of UDs from high-resolution spectra. The first attempt to determine the "true" intensities and diameters was made by Beckers & Schröter (1968). The authors applied the method of two-colour photometry to umbral photographs in two different wavelengths (blue and red). They concluded that UDs are of photospheric brightness and have diameters of 150–200 km when the appropriate corrections are applied. Koutchmy & Adjabshirzadeh (1981) later applied a similar method to a sample of 25 UDs and obtained similar results: The intensities are slightly higher than

Table 1. Photometric parameters of observed umbrae.

Umbra	AR NOAA	Date	μ	n obs.	Area (arcsec^2)	Stray light $\alpha_{\rm blue}$	Stray light $\alpha_{\rm red}$	Min. intensity $I^{\rm min}_{\rm blue}$	Min. intensity $I^{\rm min}_{\rm red}$	$T^{\rm min}_{\rm blue}$ (K)	$T^{\rm min}_{\rm red}$ (K)
a	10 459	2003-09-16	0.92	3	13.4	0.16	0.12	0.25	0.36	4930	4830
b	10 462	2003-09-16	0.87	4	33.8	0.16	0.12	0.10	0.19	4260	4240
c	10 459	2003-09-19	0.90	4	50.7	0.08	0.06	0.20	0.29	4750	4600
d	10 459	2003-09-19	0.90	4	51.3	0.08	0.06	0.13	0.19	4470	4260
e	10 463	2003-09-20	0.75	2	67.2	0.11	0.10	0.06	0.14	3970	4000

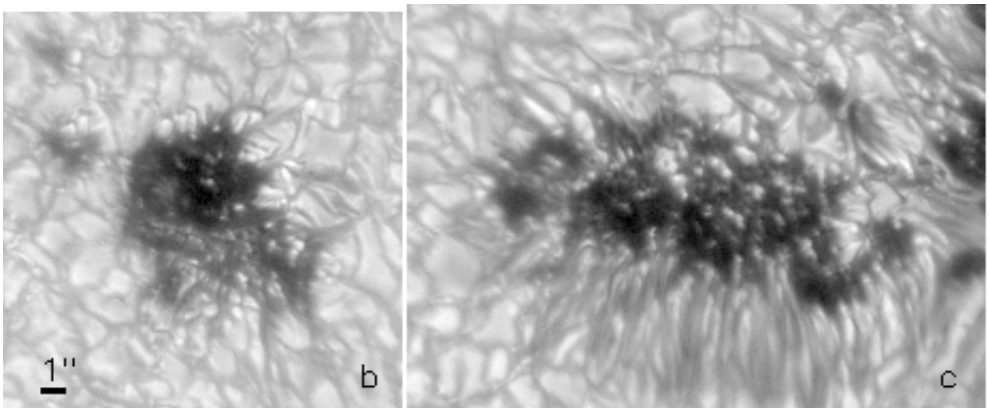

Fig. 1. Examples of observations (λ = 451 nm): Pore *b* and sunspot umbra *c*.

the mean photospheric intensity and the average diameter is 190 km. The problem of these two pioneering works was that the blue and red images were not taken strictly at the same time, so that they were influenced differently by atmospheric seeing and by possible evolutionary changes of UDs. Aballe Villero (1992) avoided this drawback and found that most of the "true" intensities are smaller than the photospheric ones and that the diameters are in the range from 100 to 400 km. From two-component semi-empirical thermal models of 10 UDs, based on spectra with spatial resolution of about 0.″5, Sobotka et al. (1993) concluded that the "true" intensity of UDs is, on average, three times higher than the intensity of the local umbral background and that the "true" diameters are typically 180–300 km.

The spatial distribution of UDs in the umbra is non-uniform. For theoretical modelling, it is important to know the average distance to the nearest neighbour and the filling factor – the ratio of the total area of UDs to the area of the umbra. Sobotka et al. (1993) reported that the nearest-neighbour distance (0.″5–0.″75) decreases and the filling factor (0.03–0.1) usually increases with increasing brightness of the umbral background.

In the present work we attempt to repeat and refine the previous measurements of intensities, diameters and spatial distribution of UDs, using observations with extremely high spatial resolution obtained with the new 1-m Swedish Solar Telescope (SST, Scharmer et al. 2003a) at La Palma.

2. Observations and data reduction

White-light images of sunspots and pores were acquired at the SST in the period 16–20 September 2003. Wavefront aberrations caused by the turbulent terrestrial atmosphere and by the telescope were partially corrected by the adaptive optics system (Scharmer et al. 2003b). Two synchronized Megaplus 1.6 10-bit CCD cameras working in frame selection mode (selection interval 20 s) recorded strictly simultaneous images in two wavelength bands: 450.75 ± 0.45 nm (blue) and 602.00 ± 1.30 nm (red). The exposure time was in the range 10–15 ms and the plate scale was 0.″041 pixel^{-1}. The signal-to-noise ratio, derived from single-exposure flatfield frames, was 100 in the blue and 200 in the red wavelength band.

Observed sunspots and pores are listed in Table 1 and two examples are displayed in Fig. 1: *a* was a small pore in a young, rapidly developing active region (AR); *b* was a large growing pore in a small AR; *c, d* were two umbral cores in a growing irregular sunspot, developed in the same AR as *a*; *e* was a stable regular sunspot.

After dark- and flat-field corrections, all intensities I in each frame were normalized with respect to the average intensity of the undisturbed photosphere $I^{\rm ph}$ to compensate for changes of transparency and/or exposure time.

Photospheric and penumbral stray light, which contaminates the umbra due to scattering in the terrestrial atmosphere, was calculated using the method developed by Martínez Pillet (1992). Parameters of the scattering phase function, composed of one Lorentzian and two Gaussians, were determined for each wavelength band from the shapes of 1′ long photometric profiles perpendicularly crossing the solar limb. Images of the limb were recorded immediately after each observation. We took into account the fact that all sunspots and pores were observed in the central zone of the disk and applied the simplified formula for stray-light contamination (cf. Eqs. (32) and (39) by Martínez Pillet 1992) $I^{\rm obs} = (1 - \alpha)\, I + \alpha$ to correct the

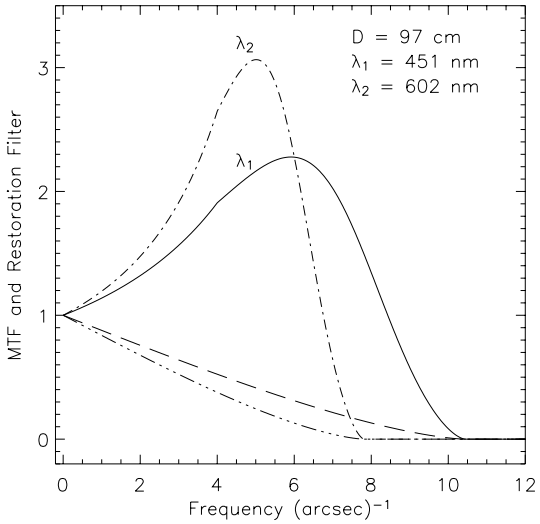

Fig. 2. One-dimensional cuts of the diffraction-limited modulation transfer functions of the 97-cm telescope (dashed for blue and dash-three-dots for red), and of the Wiener filters (solid for blue and dash-dot for red) used for image restoration.

observations. Here, $I^{\rm obs}$ and I are observed and stray-light corrected intensities in units of $I^{\rm ph}$, and α is the stray-light contamination, derived from the phase function for each wavelength and assumed to be independent of the position in the umbra. The values of α, together with the heliocentric positions μ and photometric parameters of the observed umbrae, are shown in Table 1. The level of stray light in the blue (red) wavelength band was 16 (12)% in the pores, 8 (6)% in the sunspot umbrae observed during a period of a clean sky, and 11 (10)% in the sunspot umbra observed through a light haze. We expect that the stray light was mostly of instrumental origin.

The correction for the theoretical instrumental profile of the telescope and the noise filtering was carried out simultaneously applying the two-dimensional rotationally symmetric Wiener filter (see Sobotka et al. 1999 for details) with parameters $\nu_0 = 4.0$ arcsec^{-1} and $K = 0.02$ used for both wavelength bands. The one-dimensional cuts of the resulting filters for the blue and the red, together with the corresponding MTFs, are plotted in Fig. 2. We can see from the figure that the damping of spatial information starts at distances shorter than 0.″12 (87 km at the solar surface) in blue and 0.″15 (109 km) in red, where the filter begins to be smaller than one. Taking into account the correction of wavefront aberrations by the adaptive optics, we can assume that the values shown above characterize the resolution in the best frames.

After the stray-light correction and restoration, the red-band images were aligned to the simultaneously exposed blue-band ones, taking into account the differences in plate scale (a slightly different focal length), rotation, shift and seeing-induced deformation. After this procedure, all structures in the blue and red images match with a sub-pixel accuracy.

3. Data analysis

The present analysis is based on the best n pairs of the matched blue-band and red-band images, selected for each umbra (see Table 1). In total, 17 pairs of images were analyzed. Umbral boundaries were defined visually by contours drawn in the blue images, outlining approximately the maximum intensity gradient between the umbra and its surroundings and avoiding light bridges and intrusions of penumbral filaments. Then, umbral areas were computed. Intensity minima in umbrae $I^{\rm min}$ were measured and the corresponding brightness temperatures $T^{\rm min}$ were calculated (see below). The average values are listed in Table 1. Values of $I^{\rm min}$ in individual frames differ by about ± 0.01 in units of $I^{\rm ph}$.

In the next step we estimate those umbral background intensities that would be observed in the absence of all bright small-scale structures. To do this, we first find local minima in a regular grid of 0.″41 × 0.″41 (10 × 10 pixels) subfields. The minima located inside large-scale bright features (light bridges and clusters of UDs) are removed by hand and some "minima" have to be added to reproduce correct gradients at the edges of the umbra. The umbral background is then approximated by a 2D surface fitted to the grid of the minima, using the method of thin-plate splines (Barrodale et al. 1993). In our data, the accuracy of this fit is of ± 0.03 in units of $I^{\rm ph}$. This way, we can find the approximate intensity of the umbral background $I^{\rm ub}$ at the location of an UD.

To identify UDs, a segmentation was applied to the blue- and red-band images, based on the rule that pixels with downward concavity, representing bright features, are set to 1 and the rest to 0. The obtained binary mask was multiplied by the original image, so that intensities of UDs were preserved. After the segmentation, the maximum intensity I, its coordinates, and the area A (number of pixels) was recorded for each feature. To make the identification reliable, a bright feature is considered to be an UD only if it meets the following three conditions: the intensity $I \geq I^{\rm ub} + 0.05$; the area $A \geq 9$ pixels, that is, the effective diameter $D = 0.''041\sqrt{4A/\pi} \geq 0.''14$; the position of the feature is equal for both wavelength bands. This way, 1191 UDs were identified in all 17 pairs of images.

Nearest-neighbour distances, average peak-to-peak distances of UDs and filling factors (ratio of the total area of UDs to the area of the umbra) were calculated from measured positions and areas of UDs and from umbral areas. Brightness temperatures T_λ were computed assuming the black-body radiation $I_\lambda \cdot I^{\rm ph}_\lambda(\mu) = B_\lambda(T_\lambda)$, where $B_\lambda(T_\lambda)$ is the Planck function, I_λ is the normalized observed intensity and $I^{\rm ph}_\lambda(\mu)$ is the absolute mean photospheric intensity at the heliocentric position μ. The values of $I^{\rm ph}_\lambda(0)$ are taken from Neckel & Labs (1984) and re-calculated for a given μ using the formula by Pierce (2000).

Due to their size near and possibly below the resolution limit, the observed brightness and size of UDs depend on image degradation. Although the spatial resolution of our images is very high and the effects of atmospheric seeing are partially corrected by adaptive optics, it is desirable to take advantage of the simultaneously exposed blue and red images to determine the "true" brightness and size. The method of two-colour photometry (Beckers & Schröter 1968) is based on the fact that the radiative flux coming from an UD is not influenced by image degradation.

Both the observed I_λ and "true" J_λ intensities can be expressed through the umbral background intensities ($I_\lambda^{\rm ub}$, $J_\lambda^{\rm ub}$) and the UD's surplus intensities (ΔI_λ, ΔJ_λ):

$$I_\lambda = I_\lambda^{\rm ub} + \Delta I_\lambda, \quad J_\lambda = J_\lambda^{\rm ub} + \Delta J_\lambda, \quad \lambda = \text{blue, red.} \tag{1}$$

In the following steps, we suppose (i) that $J_\lambda^{\rm ub} = I_\lambda^{\rm ub}$. This assumption is reasonable since the observed umbral background intensities are corrected for stray light and are derived from local minima situated in dark areas sufficiently large to avoid the influence of image degradation. From the flux conservation law it follows that

$$\Delta I_\lambda D_\lambda^2 = \Delta J_\lambda d_\lambda^2, \tag{2}$$

where D_λ and d_λ are observed and "true" UD diameters, respectively. We further assume (ii) $d_{\rm blue} = d_{\rm red}$. This is rather strong, because the blue and red continua originate at different geometrical heights. Taking into account Eq. (2), the colour index $c = \Delta J_{\rm blue}/\Delta J_{\rm red}$ can be calculated from the observed values: $c = (\Delta I_{\rm blue} D_{\rm blue}^2)/(\Delta I_{\rm red} D_{\rm red}^2)$. Assuming (iii) that UDs radiate like black body (a strong assumption as well), we obtain a system of two equations for the true surplus intensity $\Delta J_{\rm red}$ and for the colour temperature $T_{\rm c}$:

$$J_{\rm blue} = I_{\rm blue}^{\rm ub} + c\,\Delta J_{\rm red} = B_{\rm blue}(T_{\rm c})/I_{\rm blue}^{\rm ph}(\mu) \tag{3}$$

$$J_{\rm red} = I_{\rm red}^{\rm ub} + \Delta J_{\rm red} = B_{\rm red}(T_{\rm c})/I_{\rm red}^{\rm ph}(\mu). \tag{4}$$

The expression $B_\lambda(T_{\rm c})/I_\lambda^{\rm ph}(\mu)$ is the Planck function in units of the absolute mean photospheric intensity. The "true" diameter d is then obtained from Eq. (2).

A severe problem of this method arises from the fact that the radiation in the blue and red wavelength bands comes from different geometrical heights with different temperatures. Moreover, due to the influence of absorption lines in the blue band, the intensity is lower than that expected from Planck's law, so that the assumption (iii) is not exact. See the discussion by Tritschler & Schmidt (2002a) for more details. The two-colour photometry is also very sensitive to small errors in the measurements of I_λ, $I_\lambda^{\rm ub}$, and D_λ. In fact, the solution of Eqs. (3) and (4) was found to be inside the plausible limits $J_\lambda > I_\lambda$ and $\Delta J_{\rm red} < 2$ only for 585 UDs, about a half of the total number of measurements. For the reasons mentioned above, we consider the results of two-colour photometry to be significant only in a statistical sense and thus can be used only as a complementary information.

4. Results

The observed peak intensities of 1191 detected UDs vary in a broad range 0.16–1.24 (blue) and 0.24–1.18 (red); the intensity unit is $I^{\rm ph}$. Average intensities calculated for the whole sample are 0.53 ± 0.20 (blue) and 0.63 ± 0.18 (red). Standard deviations (1σ) characterize the scatter of individual intensities of different UDs. Average values for individual umbrae are listed in Table 2. Comparing Tables 1 and 2, we can see that UDs are brighter in umbrae with higher $I^{\rm min}$. Figure 3 demonstrates the relation between the observed intensities of UDs and local intensities of the umbral background $I^{\rm ub}$ in the blue and red bands. Pores and sunspots are represented by different symbols. The points in both scatter plots are concentrated into sector-shaped clouds, where the lower limits are determined by the UD-selection criteria. In spite of a strong scatter, we can observe a clear trend with a correlation coefficient $cc = 0.7$. Average values of the ratio $I/I^{\rm ub}$ are 1.8 ± 0.5 (blue) and 1.6 ± 0.4 (red). The ratios in individual umbrae do not depend on $I^{\rm min}$.

Average values of UD brightness temperatures in umbrae *a–e* are summarized in Table 2, together with standard deviations characterizing the scatter of individual values of different UDs. The brightness temperatures in the blue band, $T_{\rm blue}$, are

Table 2. Average observed intensities and brightness temperatures of umbral dots.

Umbra	$I_{\rm blue}$	$I_{\rm red}$	$T_{\rm blue}$ (K)	$T_{\rm red}$ (K)
a	0.58 ± 0.12	0.70 ± 0.11	5640 ± 190	5560 ± 200
b	0.48 ± 0.16	0.59 ± 0.15	5400 ± 320	5300 ± 310
c	0.59 ± 0.17	0.69 ± 0.15	5640 ± 280	5510 ± 270
d	0.56 ± 0.23	0.64 ± 0.20	5540 ± 400	5420 ± 390
e	0.38 ± 0.17	0.48 ± 0.16	5100 ± 340	5000 ± 330

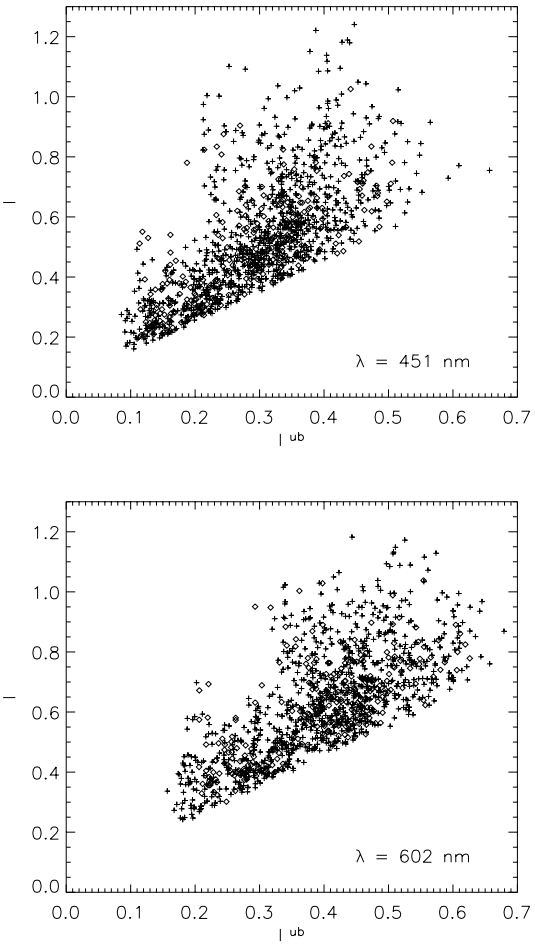

Fig. 3. Observed peak intensities I of umbral dots versus local intensities of umbral background $I^{\rm ub}$ in pores *a,b* (diamonds) and in sunspots *c, d, e* (plus signs).

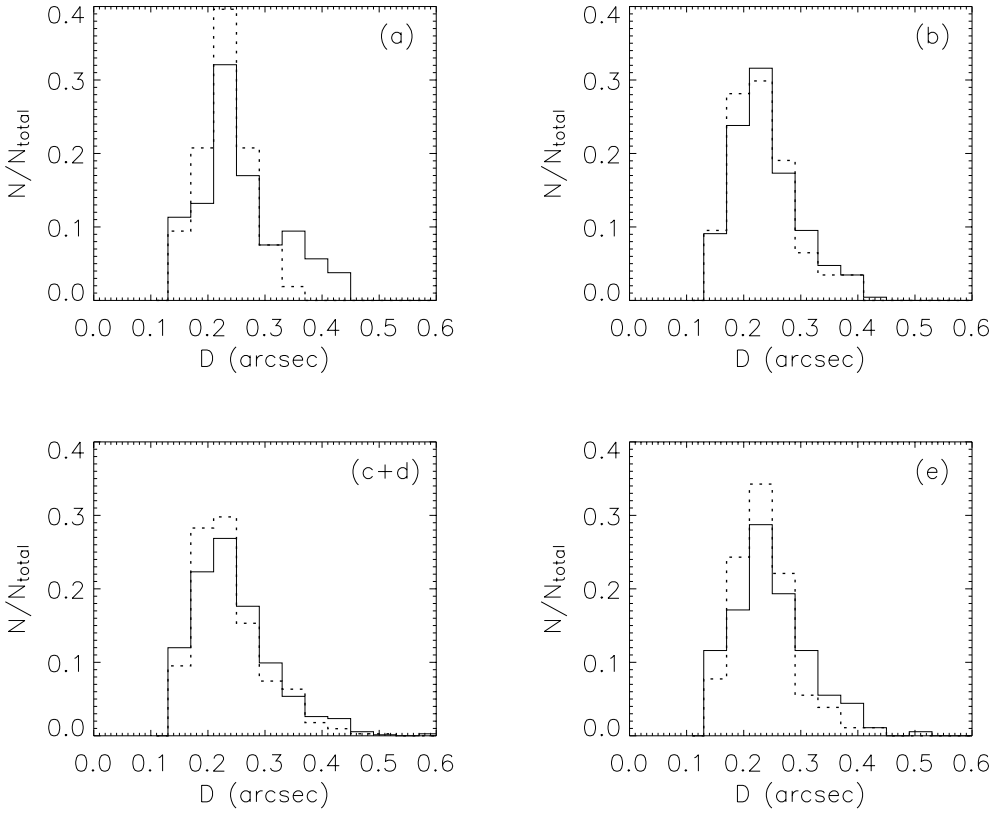

Fig. 4. Histograms of observed diameters of umbral dots in umbrae *a, b, c+d, e*. Solid line – blue band, dotted line – red band. The bin size is 0.″04, $N_{\rm total}$ = 1191.

systematically higher by 100 K than those observed in the red band, $T_{\rm red}$. This is caused by the fact that the continuum opacity is lower in blue than in red and we observe deeper and hotter layers in the blue band. The same is true also for the minimum umbral temperatures $T_\lambda^{\rm min}$ (Table 1), except for the dark and cool umbrae *b* and *e*. For comparison, in the undisturbed photosphere near the disk center, $T_{\rm blue}$ = 6300 K and $T_{\rm red}$ = 6100 K. On average, UDs are by about 1000 K hotter than the coolest area in the umbra and by 500–1000 K cooler than the undisturbed photosphere. Nevertheless, individual UDs can reach or exceed the mean photospheric brightness (see Fig. 3) and temperature but not the maximum brightness of the brightest photospheric granules (1.35 in blue and 1.25 in red).

Observed effective diameters *D* range from 0.″14 (selection limit) to 0.″6. Histograms of *D* measured in the blue and red bands in the umbrae *a, b, c+d*, and *e* are shown in Fig. 4. These histograms differ substantially from those presented by Sobotka et al. (1997) and Tritschler & Schmidt (2002b). Instead of a monotonous increase toward the smallest diameters, all histograms in Fig. 4 show a clear maximum at 0.″23 (about 170 km) that can be considered a "typical" observed size of UDs. This means that *the majority of UDs in our images are spatially resolved*. The average *D* for all 1191 UDs is 0.″24±0.″07 (175±50) km in both wavelength bands. Very similar average values of 0.″23–0.″25 are measured in the individual umbrae. Observed diameters of UDs are practically uncorrelated with the observed intensities (*cc* = 0.4), according to the previous finding by Sobotka et al. (1993).

Although the average *D* is equal in the blue and red wavelength band, many individual UDs show differences between $D_{\rm blue}$ and $D_{\rm red}$. The small differences are probably caused by residual noise in the images and large deviations appear when two or three tightly packed UDs are resolved only in one wavelength band, so that one of the resolved UDs (the rest are discarded) is coupled with an unresolved cluster in the other band.

The mean nearest-neighbour distances between UDs in the umbrae *b–e* are 0.″38–0.″42. In the small pore *a*, with only few UDs, it reaches 0.″48. The average peak-to-peak distances, derived from the number of UDs found in the unit area, are obviously larger: 0.″65 in *b, c*, 0.″76 in *d*, and 0.″82 in *a, e*. The filling factors based on observed areas of UDs are 0.11 in *b, c* and 0.08 in *a, d* and *e*. The distances and filling factors are equal for both wavelength bands.

Complementary results were obtained using the method of two-colour photometry. The solution of Eqs. (3) and (4) was found for 585 UDs, for which the differences between $D_{\rm blue}$ and $D_{\rm red}$ were small. Further we present only statistical values without distinguishing individual UDs and/or umbrae.

The calculated "true" intensities J_λ vary in a broad range of 0.2–2.8; their average is 1.2 ± 0.6 and median 1.0 for both wavelength bands. This means that about half of all 585 UDs are brighter than $I^{\rm ph}$. The number of UDs decreases with increasing J_λ. Observed and "true" intensities do not show a significant correlation (*cc* = 0.46). Also, J_λ and the corresponding local intensities of the umbral background $I_\lambda^{\rm ub}$ are

uncorrelated. Average values of $J_\lambda/I_\lambda^{\rm ub}$ are 4 ± 2 (blue) and 3 ± 1 (red), consistently with the previous result $J \simeq 3 \cdot I^{\rm ub}$ reported by Sobotka et al. (1993). Colour temperatures T_c range from 4700 K to 7800 K, with an average of 6300 ± 700 K and a median of 6200 K. The median colour temperature equals the average temperature of the undisturbed photosphere as deduced from the brightness temperatures in the two wavelength bands.

The histograms of calculated "true" effective diameters d and observed effective diameters D_λ of 585 UDs under study are shown in Fig. 5. The average of d is 0.″14 ± 0.″06 (100 ± 40 km) and median 0.″13 (95 km). For comparison, the mean free photon paths, calculated at optical depth $\tau_{5000} = 2/3$, are 90 km in the undisturbed photosphere and 70 km in sunspot umbrae and pores. The "true" and observed diameters are correlated ($cc = 0.7$) and, on average, $d/D_\lambda = 0.6 \pm 0.2$ in both wavelength bands.

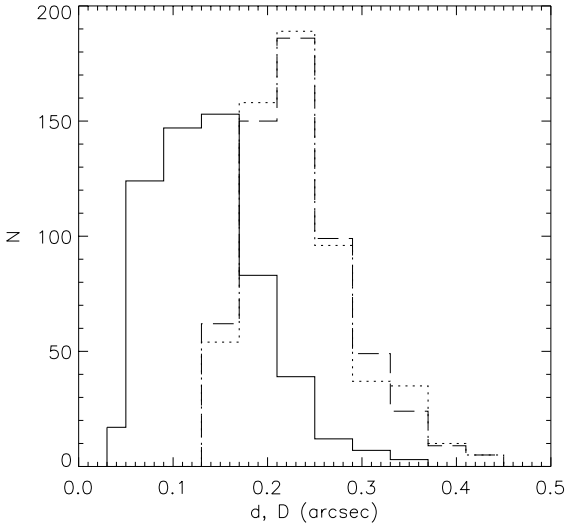

Fig. 5. Histograms of "true" d and observed D diameters of 585 umbral dots analyzed by means of two-colour photometry. Solid line – d, dashed – $D_{\rm blue}$, dotted – $D_{\rm red}$. The bin size is 0.″04.

5. Discussion and conclusions

Observed intensities, brightness temperatures, effective diameters and positions were measured for 1191 UDs detected in 17 pairs of images of two pores and three sunspot umbrae, taken in two wavelength bands: 450.75 ± 0.45 nm (blue) and 602.00 ± 1.30 nm (red). The results can be summarized as follows.

Observed intensities of UDs are correlated with local intensities of the umbral background. The average values of the ratio $I/I^{\rm ub}$, 1.8 (blue) and 1.6 (red), are greater than 1.5 (Sobotka et al. 1993) because of higher quality and spatial resolution of the images used in this study. Observed brightness temperatures of UDs are, on average, by about 1000 K higher than the coolest area in the umbra and by 500–1000 K lower than the undisturbed photosphere. Individual UDs can reach or exceed the mean photospheric brightness but not the maximum brightness of the brightest photospheric granules.

The most important result of this work is the fact that the majority of UDs are spatially resolved with the 1-m aperture telescope. In contrast to previous observations with smaller apertures, the number of UDs does not grow monotonously with decreasing observed diameter but, after reaching a maximum around 0.″23, it decreases in all observed umbrae (Figs. 4 and 5). This is not a consequence of noise filtering with the Wiener filter (Fig. 2), because the substantial suppression of contrast (filter <1) occurs only for spatial frequencies $\nu >$ 8.3 arcsec^{-1} (blue band) and $\nu > 6.7$ arcsec^{-1} (red band) that corresponds to distances 0.″12 and 0.″15. The latter value can be adopted for a very reliable and conservative resolution limit in our observations. The minimum observed diameter $D = 0.''14$ was set to accept a UD into the sample. Taking into account these facts, we see from Figs. 2 and 4 that, due to the filtering, the number of UDs can be spuriously lowered only in the first histogram bin (0.″13–0.″17) but never in the second one (0.″17–0.″21), which corresponds to the region of spatial frequencies 4.8–5.9 arcsec^{-1} with maximum image restoration. At the same time, the number of UDs in the second bin is clearly lower than that in the third bin (0.″21–0.″25) in all histograms. We can conclude that the "typical" observed size of UDs is approximately 170 km. A very similar statistical distribution of sizes, peaking at 160 km, was found by Wiehr et al. (2004) for intergranular G-band bright points observed with the 1-m SST.

The spatial distribution of UDs is non-uniform, as can be seen from the different values for the nearest-neighbour distance (0.″4) and the average peak-to-peak distance (0.″75). The nearest-neighbour distance is smaller than that published by Sobotka et al. (1993) due to the higher spatial resolution in our data. The average filling factor based on observed areas of UDs is 9%. Taking into account that the "true" diameters, calculated by two-colour photometry, are, on average, by a factor of 0.6 smaller than the observed ones (Sect. 4), the "true" areas are smaller by a factor of 0.36 and the "true" filling factor is approximately 3%.

The determination of "true" intensities and diameters of 585 UDs using the method of two-colour photometry is not very reliable, as discussed in Sect. 3. About half of these UDs have "true" intensities and colour temperatures higher than the undisturbed photosphere. This is in good agreement with the results previously obtained with this method (Beckers & Schröter 1968; Adjabshirzadeh & Koutchmy 1981). In spite of substantially better spatial resolution and the simultaneity of exposures in both wavelength bands, our new results do not differ strongly from the old ones. We cannot exclude that they are biased in the same way by some unrealistic assumptions used in the method.

Acknowledgements. The help of R. Kever and J.A. Bonet with the observations is highly appreciated. We thank the anonymous referee for many suggestions that contributed to the improvement of the paper. The 1-m Swedish Solar Telescope is operated on the island of La Palma by the Royal Swedish Academy of Sciences in the Spanish Observatorio del Roque de los Muchachos of the Instituto de Astrofísica de Canarias. This work was carried out within the framework of the grant IAA3003404 of the Grant Agency of the Academy of Sciences of the Czech Republic. A.H. thanks the Austrian Academy of Sciences for financial support. M.S. is a member of the European

Solar Magnetism Network (ESMN) supported by the EC through the Human Potential Programme.

References

Aballe Villero, M. A. 1992, Thesis, Univ. La Laguna
Barrodale, I., Skea, D., Berkley, M., Kuwahara, R., & Poeckert, R. 1993, Pattern Recognition, 26, 375
Beckers, J. M., & Schröter, E. H. 1968, Sol. Phys., 4, 303
Biermann, L. 1941, Vierteljahrschr. Astron. Ges., 76, 194
Choudhuri, A. R. 1992, in Sunspots: Theory and Observations, ed. J. H. Thomas, & N. O. Weiss (Dordrecht: Kluwer), 243
Danielson, R. 1964, ApJ, 139, 45
Denker, C. 1998, Sol. Phys., 180, 81
Hurlburt, N. E., Matthews, P. C., & Rucklidge, A. M. 2000, Sol. Phys., 192, 109
Koutchmy, S., & Adjabshirzadeh, A. 1981, A&A, 99, 111
Martínez Pillet, V. 1992, Sol. Phys., 140, 207
Neckel, H., & Labs, D. 1984, Sol. Phys., 90, 205
Parker, E. N. 1979, ApJ, 234, 333
Pierce, K. 2000, in Allen's Astrophysical Quantities, 4th edition, ed. A. N. Cox (Springer)
Scharmer, G. B., Bjelksjö, K., Korhonen, T. K., Lindberg, B., & Petterson, B. 2003a, in Innovative Telescopes and Instrumentation for Solar Astrophysics, ed. S. Keil, & S. Avakyan, Proc. SPIE, 4853, 341
Scharmer, G. B., Dettori, P. M., Löfdahl, M. G., & Shand, M. 2003b, in Innovative Telescopes and Instrumentation for Solar Astrophysics, ed. S. Keil, & S. Avakyan, Proc. SPIE, 4853, 370
Sobotka, M., Bonet, J. A., & Vázquez, M. 1993, ApJ, 415, 832
Sobotka, M., Brandt, P. N., & Simon, G. W. 1997, A&A, 328, 682
Sobotka, M., Vázquez, M., Bonet, J. A., Hanslmeier, A., & Hirzberger, J. 1999, ApJ, 511, 436
Thomas, J. H., & Weiss, N. O. 2004, ARA&A, 42, 517
Tritschler, A., & Schmidt, W. 2002a, A&A, 382, 1093
Tritschler, A., & Schmidt, W. 2002b, A&A, 388, 1048
Wiehr, E., Bovelet, B., & Hirzberger, J. 2004, A&A, 422, L63